Earth Planet. Sci. Lett. 672 (2025) 119697

Contents lists available at ScienceDirect

Earth and Planetary Science Letters

journal homepage: www.elsevier.com/locate/epsl

Lunar refractory element evidence challenges the canonical giant-impact hypothesis

Hairuo Fu *, Stein B. Jacobsen

Department of Earth and Planetary Sciences, Harvard University, Cambridge, MA 02138, USA

ARTICLE INFO

Editor: Dr O Mousis

Keywords:
Moon formation
Giant impact
Planetary differentiation
Refractory elements
Synestia

ABSTRACT

Emerging evidence of strikingly similar Earth–Moon refractory lithophile element compositions provides a key constraint on lunar origin, underscoring the need for a novel framework to test competing Moon formation models. Here, we evaluate whether the canonical giant-impact hypothesis can account for this compositional similarity. We model depth-dependent refractory element heterogeneity within the differentiated Moon-forming impactor and proto-Earth and integrate these chemical signatures with the canonical giant-impact sampling to predict the Moon's composition. Our modeling shows that the canonical model would lead to a highly fractionated proto-lunar disk composition relative toEarth's mantle and cannot reproduce the observed Earth–Moon similarity, when mantle compositional differentiation within the pre-impact bodies is considered. This result holds true irrespective of whether density-driven mantle overturn occurred in the pre-impact bodies. Instead, the observed similarity favors extensive post-impact homogenization of the proto-lunar disk, a process consistent with a high-energy giant-impact Moon formation scenario (e.g., Synestia).

1. Introduction

The giant-impact hypothesis has been the dominant paradigm for the Moon's formation since the Apollo era. The emerging debate on Earth-Moon formation focuses on the energy of the Moon-forming giant impact. Canonical low-angular-momentum giant-impact models propose that a roughly Mars-sized impactor (Theia) collided with the proto-Earth during its late accretionary stage, forming a debris disk of mixed materials from both the impactor and the proto-Earth that eventually coalesced into the Moon (Canup, 2004). In contrast, the high-angular-momentum, high-energy giant-impact hypotheses, partly motivated by the remarkable isotopic similarity of the Earth and Moon, suggest that the Moon and Earth condensed from a homogenized silicate fluid structure known as a synestia (Lock et al., 2018). The proposed high-angular-momentum scenarios include the "half-Earth" impact (Canup, 2012) and the "fast-spinning Earth" impact (Ćuk and Stewart, 2012).

The Synestia model was developed to simultaneously reconcile isotopic constraints, the Moon's volatile depletion, and experimentally determined physical properties of planetary materials (Lock et al., 2018). In this scenario, a high-energy impact produces a post-impact, supercritical fluid structure consisting of the silicate portions of the proto-Earth and impactor. As the synestia cools, a sequence of processes occurs: (i) formation of a nearly homogeneous silicate vapor disk, (ii) condensation of vapor into moonlets, which equilibrate chemically with bulk silicate Earth vapor at pressures of tens of bars, and (iii) re-accretion of the remaining vapor onto Earth, leaving the Moon in orbit with a small, captured atmosphere and beginning to cool and solidify. This evolution reproduces the Moon's Earth-like isotopic signatures, bulk composition, and volatile element pattern, shifting the problem of lunar origin from identifying a single collision geometry to achieving the conditions for a synestia.

Testing the canonical versus Synestia giant-impact models hinges in part on determining which hypothesis aligns more closely with the fundamental geochemical constraints on Earth-Moon formation. The most widely used geochemical arguments have centered on the remarkable Earth-Moon similarity in mass-independent isotope compositions, such as $\Delta^{17}O$ (Cano et al. 2020; Fischer et al. 2024; Young et al. 2016) and $\varepsilon^{50}Ti$ (Zhang et al. 2012), and radiogenic isotopic compositions such as $\mu^{182}W$ (Fischer et al., 2021; Kruijer et al., 2015). However, mass-independent isotope compositions, while distinct in bulk compositions among Solar System bodies, are generally regarded as uniform within individual bodies (Lock et al., 2020; Young et al., 2016; Zhang et al., 2012). This internal invariability limits the ability to

* Corresponding author.
E-mail address: hairuo.fu@g.harvard.edu (H. Fu).

https://doi.org/10.1016/j.epsl.2025.119697
Received 24 July 2025; Received in revised form 15 October 2025; Accepted 17 October 2025
Available online 25 October 2025
0012-821X/© 2025 Elsevier B.V. All rights are reserved, including those for text and data mining, AI training, and similar technologies.

distinguish between various Moon-formation models. For instance, the similar mass-independent isotopic signatures of the Moon and Earth can be reconciled if either (i) the final bulk silicate Earth (BSE) and bulk silicate Moon (BSM) contain near-identical contributions from Theia (Canup, 2012; Ćuk and Stewart, 2012; Hosono et al., 2019; Lock et al., 2020; Young et al., 2016; Zhang et al., 2012), or (ii) Theia and the proto-Earth shared the same bulk mass-independent isotopic compositions (e.g., Dauphas et al., 2014).

The first scenario, which involves specific mixing proportions, is a relatively weak constraint since many partial-disk-mixing impact models (Canup, 2012; Ćuk and Stewart, 2012; Hosono et al., 2019; Nakajima and Stevenson, 2015) and thorough-disk-mixing models (Lock et al., 2018) could both yield a similar Theia contribution to both the Earth and the Moon. In the second scenario, assuming isotopic similarity between Theia and the proto-Earth precludes further distinction between partial- and thorough-disk-mixing models. In other words, for any giant-impact model, the mass-independent isotope method bypasses the complexity of identifying the specific origins of lunar materials within the impactor and target mantles (i.e., from deep or shallow silicate regions), as isotopic values are largely uniform within each body. Consequently, the constraining power of this traditional isotopic proxy is limited and insufficient on its own to resolve differences between partial-mixing and high-energy, thorough-mixing models.

Thus, the Earth-Moon refractory lithophile element compositions [e.g., Ca, Al, Th, U, and rare earth elements (REEs)] may provide additional crucial constraints for testing giant-impact models, though this potential remains to be leveraged. This strength arises from the likely fractionated and heterogeneous distributions of refractory elements within the impactor and target mantles, in contrast to the mostly uniform values observed for mass-independent isotopic compositions (Fu and Jacobsen, 2024). Therefore, testing giant-impact models using refractory elements requires consideration not only of simple mixing proportions but also of the specific sampling localities from the pre-impact bodies that contributed to the lunar disk. Incorporating the effects of pre-impact mantle compositional differentiation and sampling locality introduces two new, independent dimensions of constraint. Together, these additional factors can provide a more robust framework for evaluating Moon-formation hypotheses, complementing traditional mass-independent isotope proxies.

Another strength of refractory lithophile elements, compared to volatile and siderophile elements, is that their abundances and ratios between the Earth and Moon are minimally affected by evaporation and condensation in the lunar disk and by core formation (Ivanov et al., 2022; Lock et al., 2018). This property ensures that the observed Earth–Moon compositions faithfully reflect the initial element distributions in the pre-impact bodies and their subsequent redistributions during giant-impact sampling and mixing, without introducing additional sources of fractionation.

In a recent study, we presented evidence for nearly identical abundances and ratios of refractory lithophile elements (including both major and trace elements) in the Earth's and Moon's silicate portions (Fu and Jacobsen, 2024), calling for a new-generation Moon-formation testing by leveraging this constraint. This marked consistency is a predicted outcome of the high-energy giant-impact model, which involves thorough chemical and isotopic mixing in a synestia. However, whether the canonical giant-impact model can produce such a notable similarity remains unclear. In this study, we test if the canonical giant-impact hypothesis can explain the Moon's refractory element compositions, considering the effect of magma ocean compositional differentiation in Theia and the proto-Earth.

2. Results and discussion

2.1. Chemical differentiation of Theia and proto-Earth pre-impact mantles

By the time of the Moon-forming giant impact (likely >4.5–4.4 billion years ago) (e.g., Barboni et al., 2017; Fu et al., 2023; Greer et al., 2023; Thiemens et al., 2019; Yu and Jacobsen, 2011), the hypothesized Theia and the proto-Earth likely underwent extensive internal silicate differentiation from early magma oceans (MOs) (Elkins-Tanton, 2012). Geochemical evidence for the existence and preservation of global-scale compositional differentiation is observed in various Solar System bodies with implications for early MO processes, including Vesta (Greenwood et al., 2014), the Moon (Wood et al. 1970), Mars (>4.5 Ga) (Day et al. 2024; Elkins-Tanton, 2012), and Earth (Caro et al., 2005; Carlson and Boyet, 2008; Harper and Jacobsen 1996; Hyung and Jacobsen, 2020).

We utilized the whole-mantle magma ocean crystallization sequences of Mars and Earth (bottom-up crystallization) (Elkins-Tanton, 2008) as analogs for modeling the initial compositional variations in the mantles of Theia and the proto-Earth. We also adopted present-day Mars and Earth radii and core fractions for Theia and the proto-Earth—a first-order approximation consistent with the parameter ranges used in successful canonical giant-impact simulations (e.g., Canup, 2004; Nakajima and Stevenson, 2015; Hull et al., 2024). The core radius of Theia was assumed to be the same as that of Mars (~1830 km) (Stähler et al., 2021). The bulk silicate compositions (initial MO compositions) of both bodies were assumed to be BSE-like (McDonough and Sun, 1995) because this assumption has the highest potential to lead to a BSE-like composition of the final Moon. In a later section, we also tested the results for assuming a Mars-like composition for Theia. The deep mantle of the proto-Earth was modeled as being composed of 78 wt. % bridgmanite, 18 wt. % ferropericlase, and 4 wt. % Ca-perovskite. This composition would lead to Lu/Hf and Sm/Nd fractionation patterns similar to those inferred for the early-stage evolution of Earth's deep mantle (e.g., Caro et al., 2005; Hyung et al., 2016).

We examined two potential end-member scenarios for the chemical fractionation of the MO and mantle cumulate (Supplementary Note 2). The first scenario involves a two-stage crystallization process, with equilibrium crystallization during the initial 70 % of MO crystallization, followed by fractional crystallization during the remaining 30 %. This model assumes a low mantle viscosity and a strong early thermal convection that caused early crystal suspension in the MO (Elkins-Tanton, 2012). The second scenario assumes pure fractional crystallization throughout the entire MO crystallization process (Elkins-Tanton, 2012). Our calculations revealed that the chemical fractionation of refractory lithophile elements is largely insensitive to the crystallization mode, whether hybrid or purely fractional, due to their high incompatibility. The results for pure fractional crystallization are presented in the main text, while results for two-stage crystallization are provided in the Supplementary Material, Figs. S1–S5..

In Fig. 1, we illustrate the modeled refractory major element concentrations in the mantle cumulate of Theia and the proto-Earth as a function of radius (Mg, Si, and Fe are moderately refractory elements). Increasing Fe/Mg and Ca/Al ratios toward the outer silicate portion of both bodies are expected due to the high compatibility of Mg in olivine and pyroxene and Al in majorite and garnet. An overall continuous enrichment of Ca toward the upper mantle is a consistent feature for both bodies.

In Fig. 2, we present the calculated refractory trace and major element fractionation as a function of degree of MO crystallization. A first-order similarity between the proto-Earth and Theia mantle is the prominent enrichment of incompatible lithophile elements in the remaining MO and the fractionating mantle cumulates as crystallization progresses (Fig. 2). Sr, Ti, and Eu exhibit slightly positive anomalies compared to other highly incompatible elements, such as Th and U. Additionally, the proto-Earth's residual MO composition shows greater

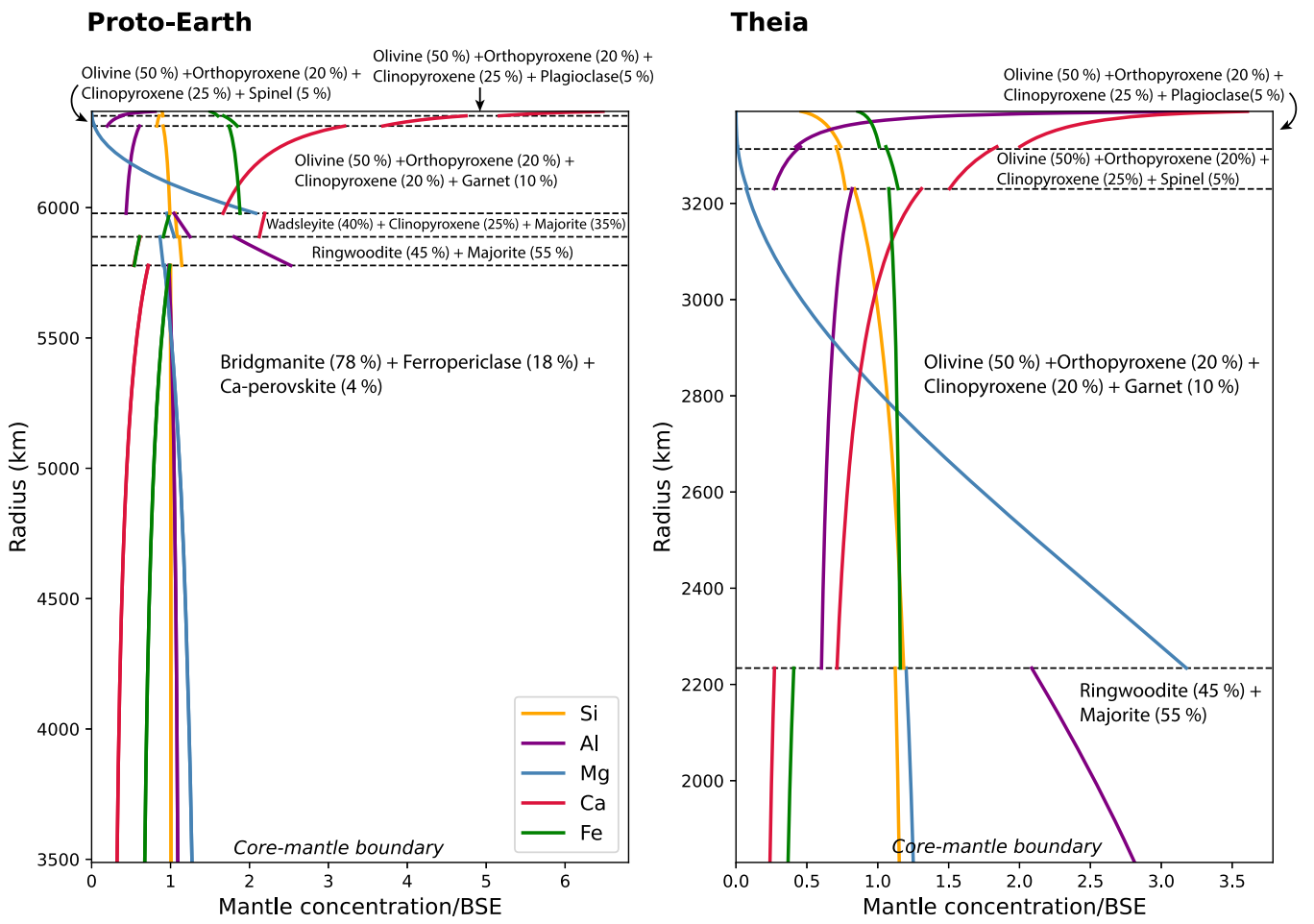

Fig. 1. Proto-Earth and Theia bottom-up magma ocean crystallization sequences and refractory major elements distribution in the mantle. Mineral proportions (in weight percent) are adapted from Elkins-Tanton (2008). The bulk silicate chemical compositions (bulk MO composition) of Theia and the Proto-Earth are assumed to be both BSE-like (McDonough and Sun, 1995). Element variations are normalized to the BSE values. The surface radii of the proto-Earth and Theia are set to 6378 km and 3396 km, respectively, while their core-mantle boundary radii are 3488 km and 1830 km, respectively. The results illustrate pure fractional crystallization of the magma ocean without mantle overturn.

REE fractionation, due to the possible fractionation of Ca-perovskite in the deep mantle.

We used element ratio pairs (Al/Ca, Mg/Fe, La/Lu, and Sr/Th) to demonstrate mantle compositional heterogeneity in the proto-Earth and Theia (Fig. 3). Mixing between these silicate reservoirs and between the two bodies should determine the expected chemical compositions of the BSM under canonical giant-impact models. The BSM is observed to have a near-chondritic ratio and an Earth-like refractory element enrichment (~2.7 times CI chondrite) (Fu and Jacobsen, 2024; Taylor and Wieczorek, 2014), both serving as critical benchmarks for comparison. By definition, the observed BSM composition can be matched if the giant impact samples all the various mantle reservoirs evenly (e.g., samples the average bulk composition) from each body to make the lunar disk material. However, if a sampling bias exists—particularly one associated with most canonical giant-impact models (Canup, 2004), the silicate compositions sourced from either body would become chemically fractionated, leading to a predicted BSM composition that likely diverges from observations. A "shallow-provenance bias" is known for the canonical giant-impact models (Canup, 2004; Warren, 2005), characterized by preferential sampling of the outer portions of the impactor and target to explain the Moon's iron depletion (~2 wt. % core mass) (e.g., Khan et al., 2006).

2.2. *Depth-dependent sampling probability of mantles and cores in a canonical giant impact*

The canonical models with mixing ratios of 70 % to 90 % between Theia and the proto-Earth mantle are well-documented (Canup and Asphaug, 2001; Canup, 2004; Hull et al., 2024; Nakajima and Stevenson, 2015). However, these studies did not report detailed depth-dependent sampling profiles of the mantles. In the absence of high-resolution depth sampling data, we parameterized multiple sampling probability profiles to approximate depth-dependent sampling in canonical giant-impact models.

The four parameterized sampling models are shown as functions of radius (r) in Figs. 4 and 5. They were designed to encompass possible outcomes of canonical giant impacts. Model 1 assumes strong preferential sampling of surface materials over deeper materials (Fig. 4A). Model 4 assumes aggressive sampling of the deeper mantle (Fig. 4D). Models 2 and 3 represent intermediate scenarios (Figs. 4B–C). In all cases, the sampling probability is normalized to a maximum of unity at the surface.

For Theia, canonical giant-impact models suggest sampling extends to the outer portion of Theia's core (Canup, 2004). The one-dimensional sampling probability (Fig. 4A–D) was converted into spherical surface-area-weighted sampling probabilities by multiplying by r^2 (Fig. 4E–H). The cumulative density function (CDF) of this profile yields the cumulative volume proportions sampled below a given radius

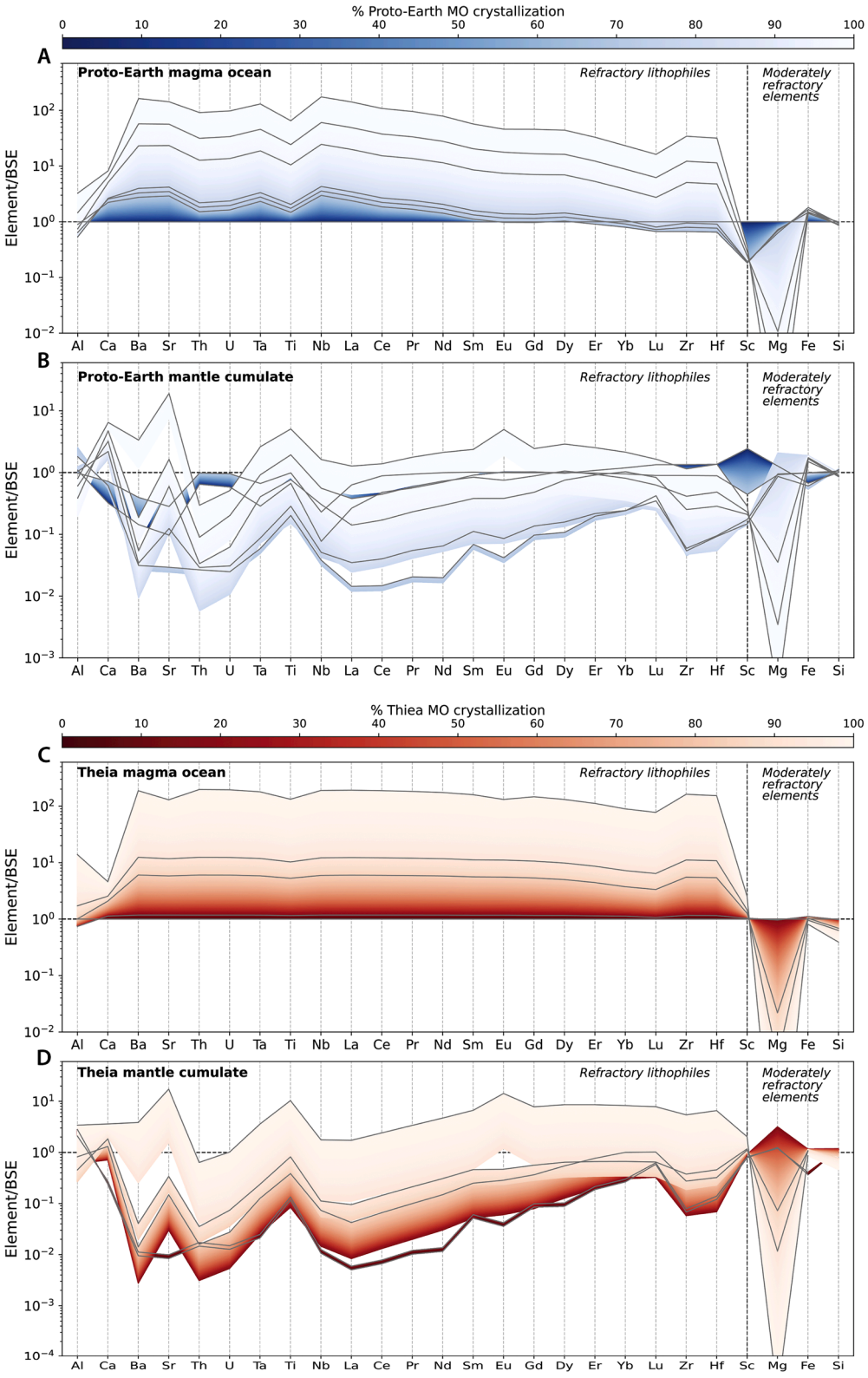

Fig. 2. Refractory elements fractionation in the evolving magma oceans and mantle cumulates. The dashed horizontal black lines represent the BSE-normalized initial magma ocean (MO) composition, which also reflects the bulk silicate composition. The evolving element compositions are color-coded according to the corresponding degree of MO crystallization. The gray fine lines delineate the MO crystallization stages corresponding to Fig. 1A & B. The results illustrate pure fractional crystallization of the magma ocean.

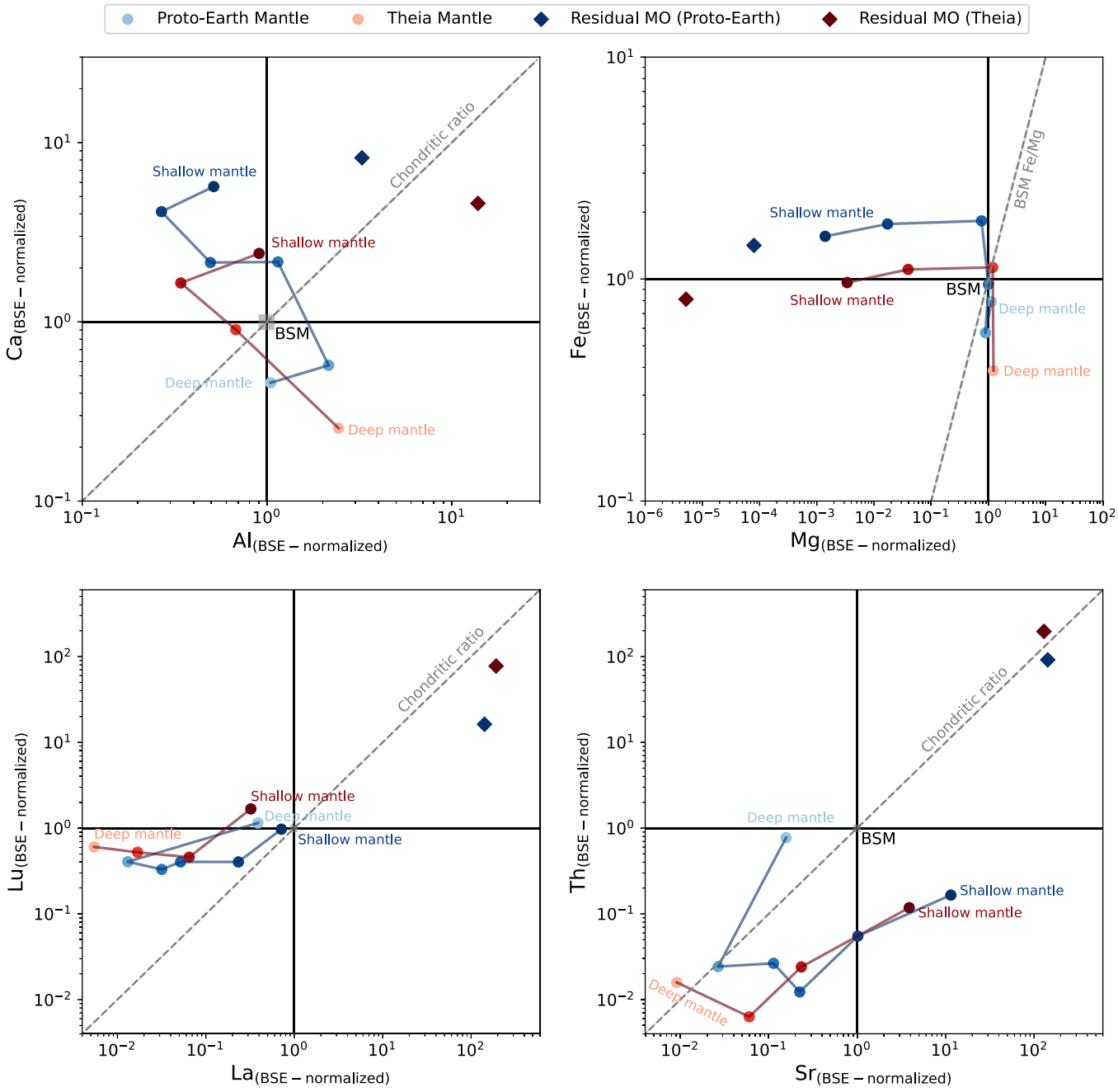

Fig. 3. Modeled mean refractory-element compositions of the various mantle reservoirs of Theia and the proto-Earth. The intersection of the black lines at unity and the shaded box marks the observed BSM values (assumed equivalent to BSE) with ~10 % relative uncertainty (Fu and Jacobsen, 2024; Taylor and Wieczorek, 2014). The dashed 1:1 line indicates the chondritic ratio for BSM refractory elements, whose uncertainty is at most ~2 % (Alexander, 2019a, 2019b); the proposed BSM Fe/Mg ratio is likewise within ~5 % of unity (Schmidt and Kraettli, 2022, and references therein). These uncertainty envelopes are too small to be visible at the scale of the diagram. The results illustrate pure fractional crystallization of the magma ocean and show that preferential sampling of the shallow mantle is unlikely to reproduce the BSM compositions.

(Fig. 4I–L). To match the Moon's ~2 wt. % final core mass, the core mass sampled from Theia cannot exceed ~3 wt. % of the total sampled Theia's materials because (i) the lunar core is sourced primarily from Theia's core (according to the canonical giant-impact dynamics), and (ii) Theia's materials constitute >70 % of the lunar disk (Canup, 2004). Given the higher density of Theia's core (~5500 kg/m^3) (Khan et al., 2006) compared to average silicates (~3346 kg/m^3) (Wieczorek et al., 2006), the sampled core volume should not exceed ~1.5 % of the total sampled materials. Accordingly, we implemented a constraint allowing only 1 % to 2 % of Theia's core volume to be sampled across all four models. Using a Monte Carlo approach, the sampling probability profiles were parameterized to match this range (Fig. 4I–L) and to best mimic canonical giant-impact simulation results.

2.3. *Predicted lunar refractory element compositions under canonical giant-impact models*

The depth-dependent sampling probabilities for Theia and the proto-Earth were combined with their mantle chemical fractionation profiles using a Monte Carlo approach to determine the bulk chemical composition that each body contributes to the lunar debris disk (Supplementary Note 4). Mixing proportions, representing the percentage of the

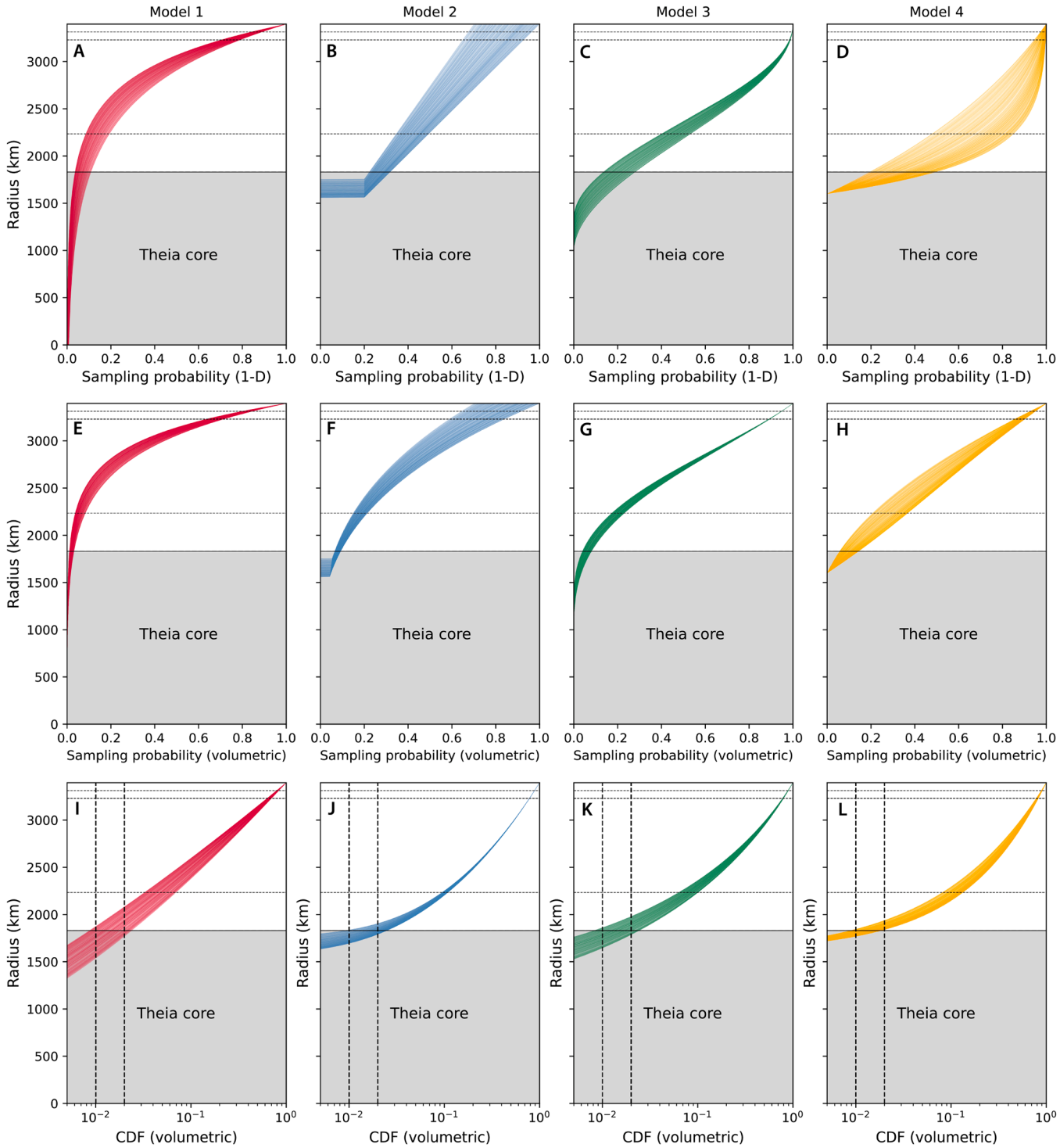

Fig. 4. Depth-dependent sampling models (Models 1 to 4) for Theia materials contributing to the lunar disk in a canonical giant impact. The first row (A–D) represents one-dimensional relative sampling probabilities as a function of depth during a giant impact. The second row (E–H) depicts the spherical surface-area-weighted sampling probabilities at various radii. The third row (I–L) shows the cumulative density function (CDF) of the second row, representing the cumulative volume fraction sampled beneath a given radius. For all four sampling models, to account for the Moon's small core fraction (~2 wt. %), the CDF at Theia's core-mantle boundary (I to L) must fall within the range of ~1 % to 2 % (bounded by the vertical dashed lines). The horizontal dotted lines correspond to the magma ocean crystallization stages delineated in Fig. 1B.

Moon sourced from Theia (ranging between 70 % and 90 %), were randomly sampled based on the proposed range for successful canonical giant impacts (Canup, 2004). These proportions were then used to calculate the predicted mean refractory element compositions of the debris disk. We assumed complete homogenization of the debris disk, resulting in a composition equivalent to that of the BSM.

We further compared the predicted BSM element compositions under canonical giant-impact models with the observed BSM values to assess consistency. Fig. 6 presents the results for the element proxies first introduced in Fig. 4. In each plot, the symbols represent the predicted BSM compositions derived from the sampling models, while the color gradient indicates Theia's mass contribution to the proto-lunar disk. A

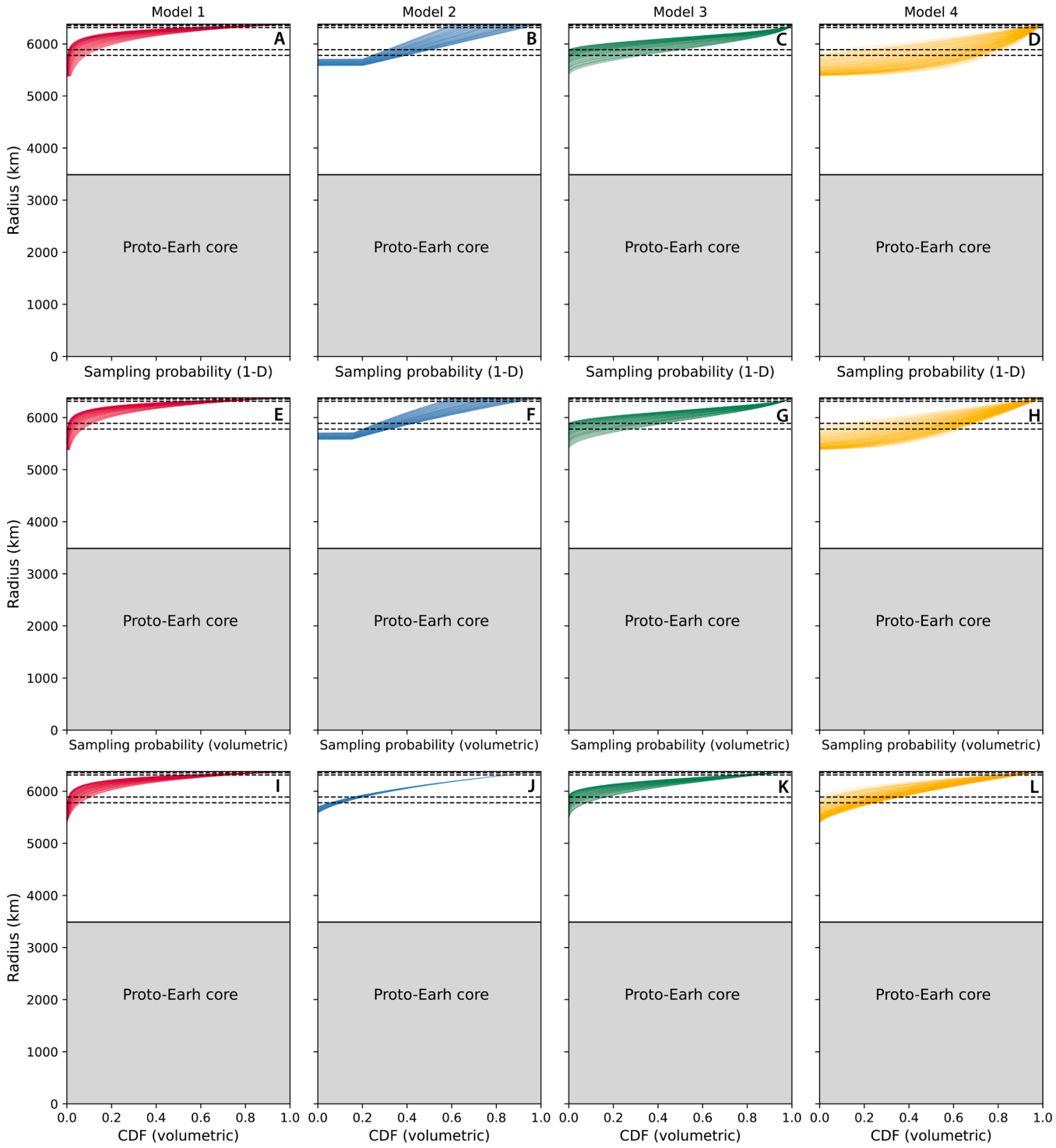

Fig. 5. Depth-dependent sampling models (Models 1 to 4) for proto-Earth materials contributing to the lunar disk in a canonical giant impact. The first row (A–D) represents one-dimensional relative sampling probabilities as a function of depth during the impact. The second row (E–H) depicts the spherical surface-area-weighted sampling probabilities at various radii. The third row (I–L) shows the cumulative density function (CDF) of the second row, representing the cumulative volume fraction sampled beneath a given radius. For the proto-Earth, materials beneath a depth of ~1000 km (corresponding to a radius of 5378 km) remain unsampled (Canup, 2004). The horizontal dotted lines correspond to the magma ocean crystallization stages delineated in Fig. 1A.

total of 1000 simulations were performed for each sampling model. The BSM refractory element abundances are estimated to match those of the BSE, with an approximate ~10 % uncertainty (Fu and Jacobsen, 2024; Taylor and Wieczorek, 2014). The BSM refractory element ratios are assumed to be chondritic, with a maximum uncertainty of 2 %, based on observed variations in chondrites (Alexander, 2019a, 2019b).

For element concentration comparisons, the results reveal an overall poor match between model predictions and observations, with less than 5 % overlap for any element proxy. Major element proxies (e.g., Ca, Al, Fe, and Mg) (Fig. 6A & B) show a slightly better match compared to highly incompatible trace elements (e.g., La, Lu, Sr, Th), likely due to the smaller initial heterogeneity in the pre-impact mantle (Fig. 2). For

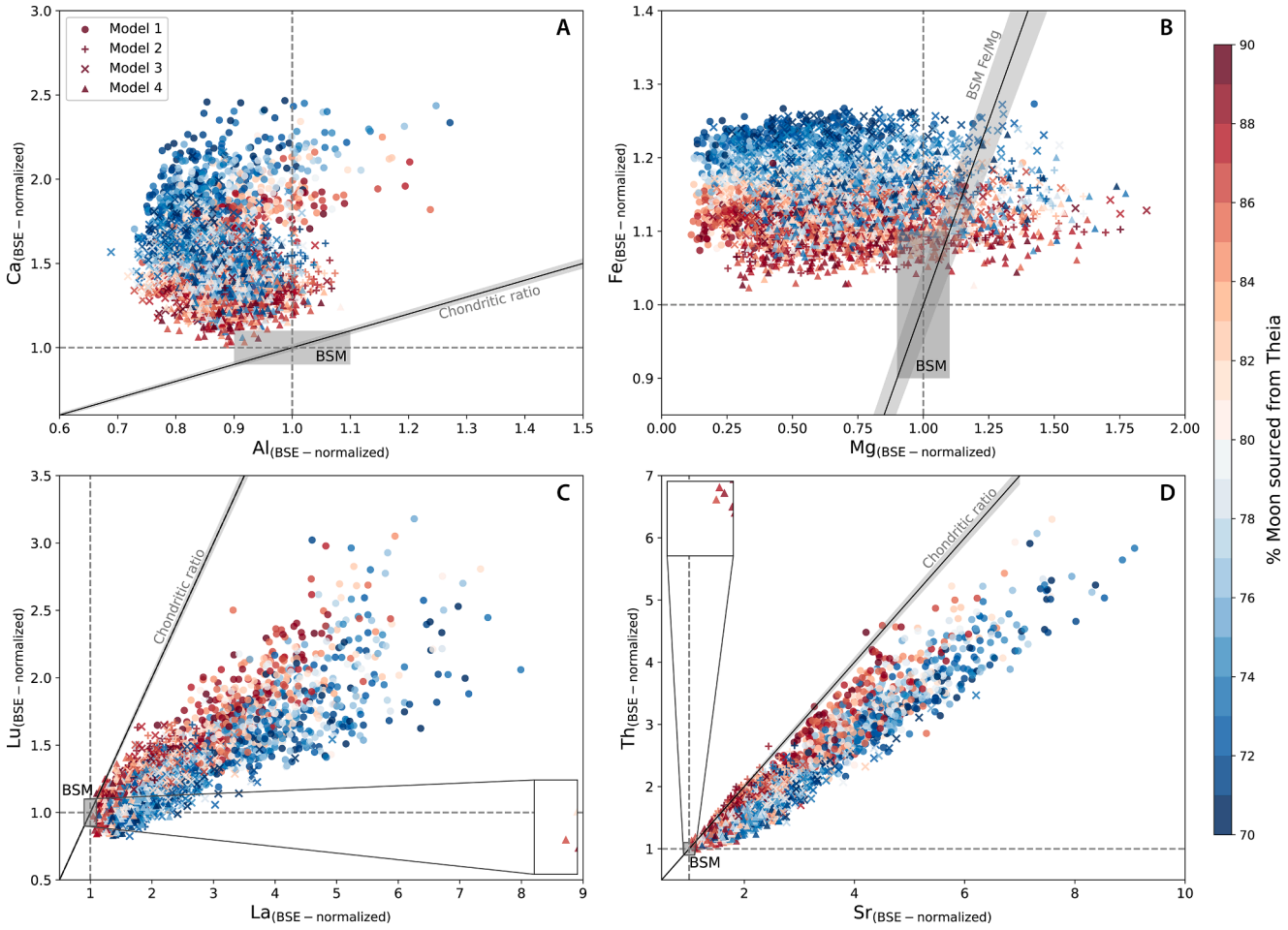

Fig. 6. Predicted BSM refractory element compositions for the canonical giant-impact model compared to lunar observations. The gray box represents the observed BSM concentrations, which are similar to those of the BSE and include a ~10 % uncertainty (Fu and Jacobsen, 2024; Taylor and Wieczorek, 2014). Symbols indicate the modeled BSM compositions derived using individual sampling models (Models 1 to 4) (Figs. 4 and 5), with 1000 samples for each model. The color gradient reflects the proposed mass fraction of the BSM sourced from Theia (~70 % to 90 %) (Canup, 2004). The 1:1 slopes and shaded regions indicate the chondritic ratio or Fe/Mg ratio proposed for the BSM, along with their uncertainties [~2 % for the chondritic ratio (Alexander, 2019a, 2019b) and ~5 % for the Fe/Mg ratio (Schmidt and Kraettli, 2022, and references therein)]. The results reveal an overall poor match between the model predictions and observations, with less than 5 % overlap for any pair of elements, demonstrating the difficulty of obtaining the BSM composition using the canonical model of Moon formation.

element ratio comparisons, most modeling results exhibit highly non-chondritic element ratios, attributed to the combined effects of shallow-provenance sampling and pre-existing chemical differentiation in the pre-impact mantles.

A more thorough model-data testing can be achieved by integrating the complete refractory element model predictions with the lunar observations, forming a multi-dimensional test (Fig. 7). The predicted enrichment of refractory elements and fractionated element ratios is a consistent feature across all sampling models, with the extent of these effects being sensitive to the mixing proportions between Theia and the proto-Earth mantle. Interestingly, a closer match seems to be reached when (i) a significant portion of Theia's deep mantle is sampled (Model 4, Fig. 4D) and (ii) the lunar disk is composed of >85 % material sourced from Theia. Nevertheless, despite the modeled BSM concentrations being closer to lunar constraints in Model 4, the refractory element ratios remain highly fractionated from the near-chondritic ratios (Fig. 7D and Fig. 8D), excluding a feasible match. In addition, exceptionally high proportions of Theia-derived material in the disk (>85 %) would increasingly conflict with the mass-independent isotopic evidence, which necessitates the disk to be predominantly composed of the proto-Earth mantle (assuming Theia and the proto-Earth carried distinct values preceding the impact) (Canup et al., 2023; Lock et al., 2020; Young et al., 2016). This apparent conflict between refractory-element and traditional isotopic evidence challenges efforts to reconcile the Moon's composition with the canonical giant-impact scenario.

For each simulation associated with each sampling model (Models 1 to 4), we calculated a joint probability of matching the modeled results with all BSM refractory element constraints simultaneously (for both element concentrations and ratios, Figs. 7 and 8) (Supplementary Note 4). Although our preferred BSM refractory element concentrations are within 10 % of the BSE values (Fu and Jacobsen, 2024), other studies considered wider ranges, with concentrations ranging from 0.8 to 1.7 times BSE values (Kronrod et al., 2018; Taylor, 1982; Taylor and Wieczorek, 2014). For the hypotheses of a refractory-element-enriched Moon (from 1.5 to 1.7 times BSE values) (Taylor, 1982; Kronrod et al., 2018), it is unclear how such an enrichment can be achieved during the Moon formation. The combined effect of lunar core formation (2 wt. % of the Moon) and lunar major volatile element depletion (such as Na and K) would enrich refractory elements by up to a few percents in the BSM; yet the enriched hypothesis requires a 50 % to 70 % enrichment, which are challenging to explain. We have also found that the enrichment hypotheses, based largely on the Al content of Moon, are inconsistent with the evidence from refractory trace elements of the Moon (Fu and Jacobsen, 2024). Nevertheless, we want to explore how a wider range of assumed BSM compositions would affect the results and conclusions.

For testing purposes only, we take a broad lunar refractory element

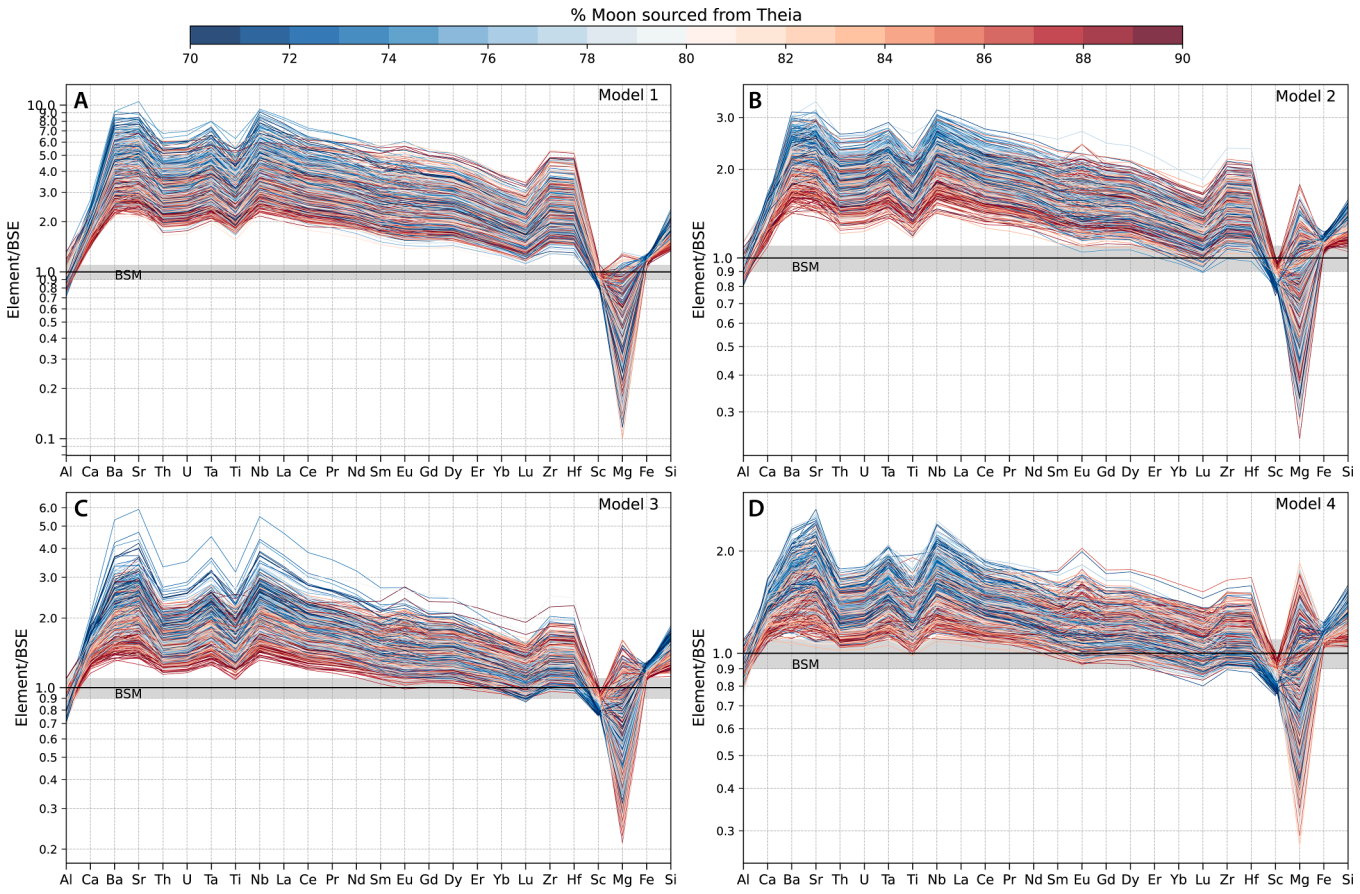

Fig. 7. Comparison of complete refractory element compositions between the canonical giant-impact predictions and lunar observations. The y-axis data show the modeled element concentrations of the BSM normalized by the BSE values. The horizontal line and shaded envelope represent the observed BSM composition, which is consistent with the BSE and with a ~10 % uncertainty (Fu and Jacobsen, 2024; Taylor and Wieczorek, 2014). Each panel corresponds to results derived from a specific sampling model, as shown in Figs. 4 and 5. Each color-coded curve (1000 curves per panel) represents one simulation of the modeled BSM element composition based on the percentage of the Moon's material sourced from Theia. The predicted highly fractionated BSM compositions demonstrate the difficulty of explaining the Moon's composition by the canonical model.

composition estimate, with concentrations ranging from 0.8 to 1.7 times BSE values (Fu and Jacobsen, 2024; Kronrod et al., 2018; Taylor, 1982; Taylor and Wieczorek, 2014). For the BSM refractory element ratios, we take them to be the same as the BSE (Fu and Jacobsen, 2024; McDonough and Sun, 1995), with a maximum of 5 % relative uncertainty (defined by the Fe/Mg ratio uncertainty in the BSM) (Schmidt and Kraettli, 2022 and references therein). Fig. 9 presents the cumulative density functions (CDFs) of the joint match probability for the four sampling models, assuming both two-stage and pure fractional crystallization of the pre-impact mantles. The two-stage MO crystallization process (equilibrium crystallization followed by fractional crystallization), which might be expected to reduce initial mantle heterogeneities and improve match probabilities, yields improvements over the pure fractional crystallization model but does not lead to a substantial match with the observations either. The low cumulative match probabilities ($<10^{-3}$) highlight the difficulty of reconciling the Moon's fundamental refractory element compositions with the canonical giant-impact model, regardless of the assumed sampling, BSM compositional uncertainty, or chemical differentiation models—even when assuming that Theia and the proto-Earth shared the same bulk chemical composition.

2.4. Testing a Mars-like Theia composition and its effects

For the calculation above, we assume that Theia and the proto-Earth shared the same bulk chemical composition (same as the BSE). This choice stems from our belief that a BSE-like Theia provides the best opportunity for the canonical giant-impact model to possibly match the observed BSE-like Moon's composition. Nevertheless, dynamical and isotopic evidence suggests that Theia might have originated from outer Solar System (Brien et al., 2014; Budde et al., 2019) with a bulk chemical composition possibly similar to Mars. Therefore, we do not exclude such a possibility and performed a simulation that assumes an initially Mars-like Theia composition (Yoshizaki and McDonough, 2019) (Supplementary Note 5).

Similar to our expectation, the simulation suggests that assuming a Mars-like Theia composition does not make the canonical giant impact yield a closer match to the observed lunar refractory element compositions (Figs. S8 and S9). Particularly, from a major element perspective, the substantially higher Fe content (14.7 wt. %) and relatively lower Ca and Al contents of the bulk silicate Mars would lead to even more fractionated Fe/Mg and Ca/Al ratios of the lunar disk and a worse comparison with the observed lunar range (Fig. S7). Integrating the full element concentration and ratio constraints yields slightly worse match probabilities (Fig. S10) compared to the model that assumes a BSE-like Theia (Fig. 9). This test aligns with the prediction that a non-BSE-like Theia composition makes it even harder for the canonical giant-impact model to explain the observed lunar refractory element signatures.

2.5. Testing density-driven mantle-overturn effects

In the scenario above, we have assessed the results assuming the pre-impact mantles preserved the chemical heterogeneity from bottom-up

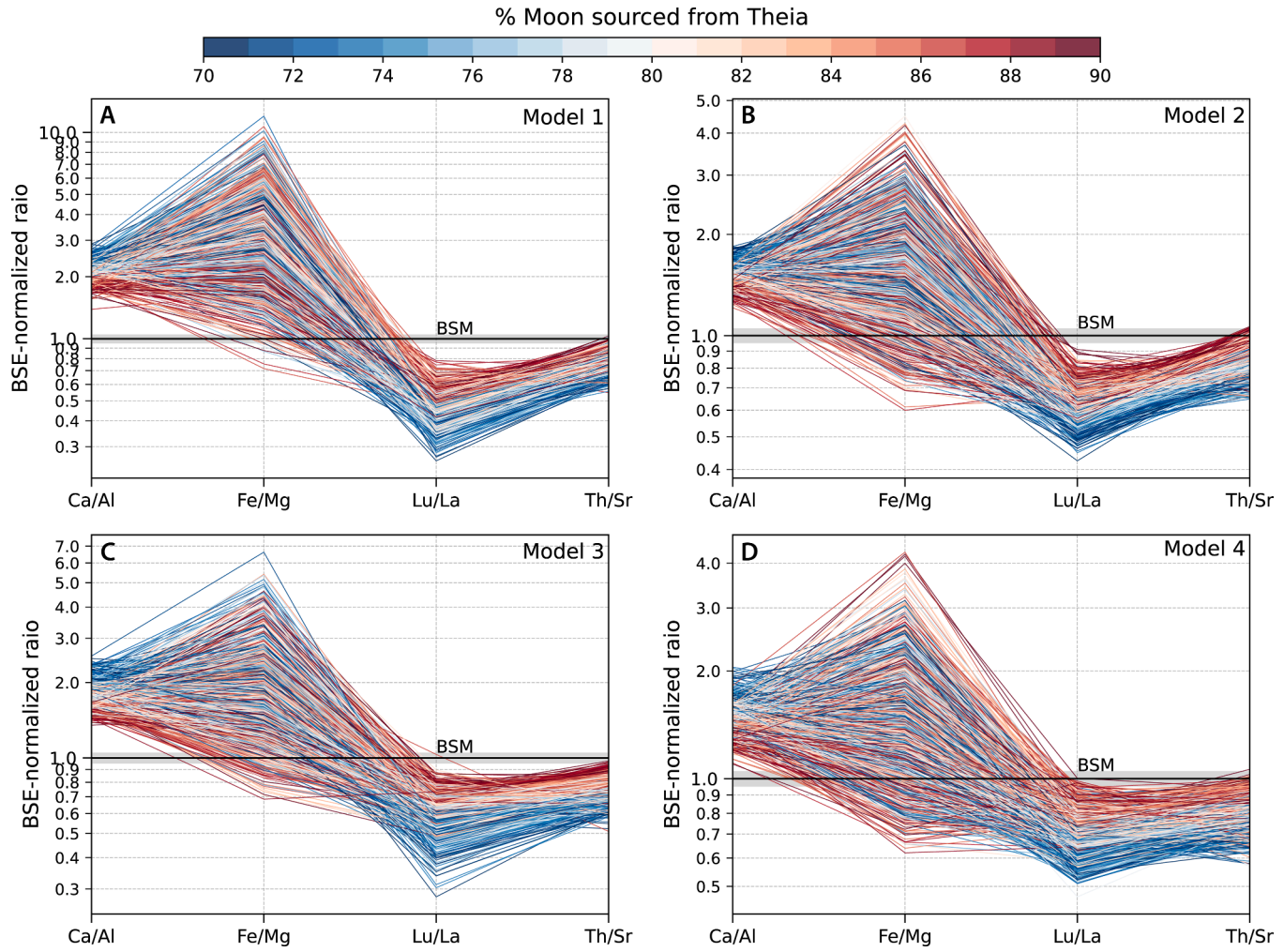

Fig. 8. Comparison of refractory element ratios between the canonical giant-impact predictions and lunar observations. The y-axis data show the modeled element ratios of the BSM normalized by the BSE values. The horizontal line and shaded envelope represent the chondritic ratio with a maximum of ~5 % uncertainty. Chondrites have a typical refractory element ratio variation of 2 %, but the Fe/Mg ratio in the BSM has a maximum of 5 % uncertainty. Therefore, we adopt 5 % as the maximum uncertainty in the refractory element ratio. Each panel corresponds to results derived from a specific sampling model, as shown in Figs. 4 and 5. Each color-coded curve (1000 curves per panel) represents one simulation of the modeled BSM element composition based on the percentage of the Moon's material sourced from Theia. For all sampling models, the canonical giant impact would predict highly fractionated element ratios that are incompatible with the lunar observations.

MO crystallization. However, due to a predicted increasing Fe/Mg ratio in the residual magma ocean and the fractionating minerals in the late MO stage, the later-formed cumulate may become denser and lead to a density-driven overturn of the mantle, causing redistribution of the element heterogeneity (e.g., Boukaré et al., 2018; Elkins-Tanton et al., 2003; Hess and Parmentier, 1995). The possibility of mantle overturn has been hypothesized for various-sized Solar System objects including the Moon (Hess and Parmentier, 1995), Mars (Elkin-Tantons et al., 2003), and Earth (Boukaré et al., 2025). In the fractional crystallization scenario, our modeling also suggests overall increasing Fe/Mg ratios in the MO and cumulates as the MO crystallizes (Fig. S11), pointing toward a mantle overturn possibility.

To test this possible scenario, we performed calculations by considering efficient mantle overturn developed within the proto-Earth and Theia mantles (Supplementary Note 6). Our results show that the final lunar-disk composition derived from overturned pre-impact mantles are highly depleted in refractory element concentrations and fractionated in element ratios (Fig. 10). The magnitudes of element depletion and ratio fractionation are similar across all four giant-impact-driven sampling models (Fig. 10). The elemental fractionation patterns in the mantle-overturn scenario (Fig. 10) are complementary to the scenario where mantle overturn is not invoked (Fig. 7). Especially, the extent of element ratio fractionation (the deviation from the chondritic ratio) is even stronger in the mantle-overturn case (Fig. 10) compared to the no-overturn hypothesis (Fig. 7). These results show that assuming mantle overturn in the pre-impact bodies does not improve the match between the canonical giant-impact hypothesis and the observed Earth-Moon refractory element similarity. In fact, if one considers a more refractory element-enriched Moon (1.5–1.7 times BSE values) (Kronrod et al., 2018; Taylor, 1982), the depleted element abundance predicted in the mantle-overturn case would make it even harder to explain the lunar composition in the context of a canonical giant impact.

Furthermore, how mantle overturn occurred or how soon it occurred in the pre-impact bodies depend on more than just the composition-dependent density of liquids and solids. From a mantle dynamics perspective, solid-state thermal convective mixing and density-driven overturn might have developed concurrently with ("early" convection) or shortly after MO crystallization ("late" overturn), possibly promoting early mixing of the compositional layers (Boukaré et al., 2018). The exact overturn scenarios for Theia and the proto-Earth depends on factors such as the MO crystallization timescale relative to mantle viscosity, which likely differ between various bodies, and the timing of the

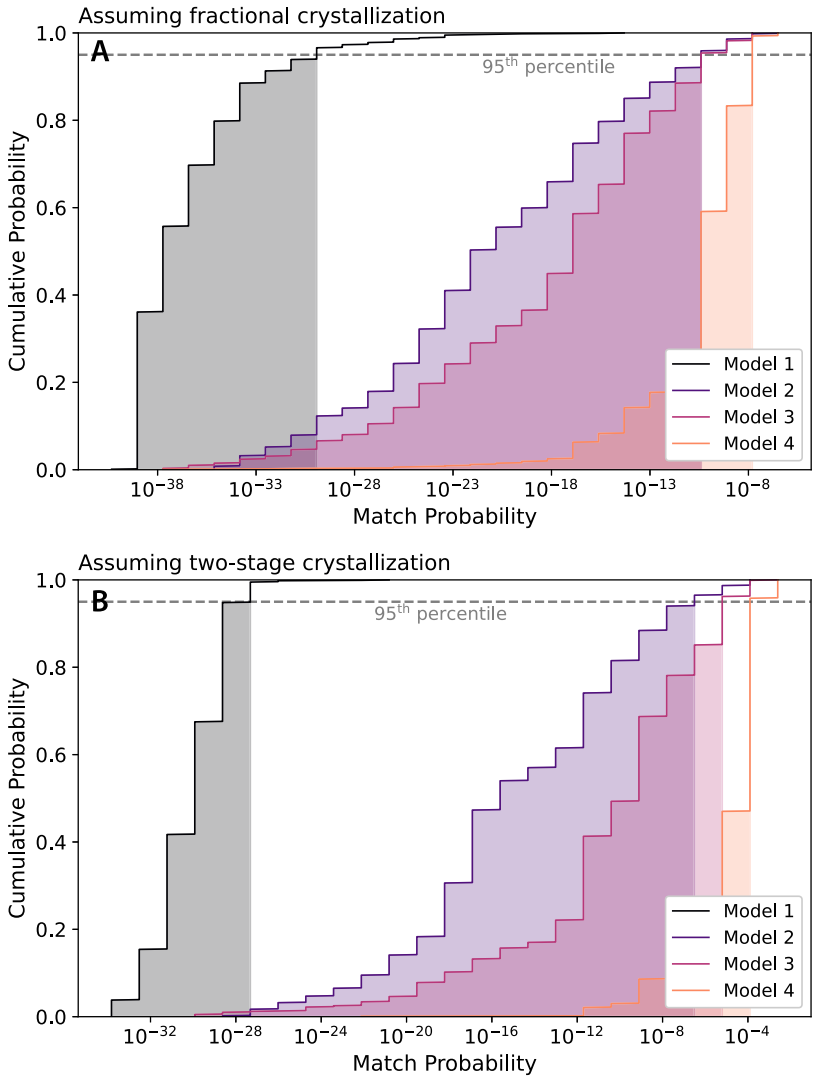

Fig. 9. Cumulative distribution functions (CDFs) of the match probability between canonical giant-impact predictions and lunar observations. The upper panel shows results assuming pure fractional crystallization of the mantles in the pre-impact bodies, while the lower panel depicts results assuming two-stage crystallization (70 % equilibrium crystallization followed by 30 % fractional crystallization). For each sampling model (Models 1 to 4), the match probability of each simulation and the CDF of 1000 simulations are calculated based on the results from Fig. 7 (fractional crystallization) and Fig. S5 (two-stage crystallization). The shaded regions for each sampling model represent the 95th percentile of the match probability. All 95th percentiles fall below 10^{-3}, demonstrating a poor match between canonical giant-impact predictions and lunar observations.

Moon-forming impact (Boukaré et al., 2018; Elkins-Tanton, 2008, 2012). A recent study (Boukaré et al., 2018) shows that early-convection and late-overturn scenarios would yield similar radial compositional heterogeneity, yet the early-convection case would increase lateral compositional heterogeneity. To first order, our current modeling results for the mantle-overturn scenario, which adopt the mean radial composition in the pre-impact mantle, are applicable for both the early-convection and late-overturn cases.

A further resolution of the mantle overturn effects could rely on better understanding the early mantle compositional heterogeneity evolution as a function of time. The time-dependent mantle composition variations, paired with the timing of Moon-forming giant impact, could potentially provide a more comprehensive synthesis of the possible lunar-disk compositions resulting from the canonical giant-impact hypothesis. If the canonical giant impact occurred at a time when some early mixing effectively reduced radial heterogeneity in both pre-impact mantles, an increase in the match probability for canonical giant-impact models with observed lunar compositions could be expected. As such, the required level of pre-impact mantle homogenization to align with the canonical giant-impact models can be rigorously evaluated in future studies. However, the feasibility of achieving the desired extent of early compositional mixing in both pre-impact bodies must be independently examined through (i) geodynamical modeling and (ii) geological evidence, which suggests the pervasive preservation of early compositional differentiation in differentiated bodies (Carlson and Boyet, 2008; Caro et al., 2005; Day et al., 2024; Elkins-Tanton, 2012; Greenwood et al., 2014; Hyung and Jacobsen, 2020). The preservation of early mantle heterogeneity may be especially stronger for a Mars-sized body (Theia) due to its potentially slower mantle mixing rate compared to an Earth-sized body (Jacobsen and Yu, 2015), evidenced by preserved $^{182}W/^{183}W$ and $^{142}Nd/^{144}Nd$ heterogeneities up to the present (Jacobsen and Yu, 2015). As a result, because the lunar disk sources mostly from the impactor's materials in a canonical giant impact and the giant impact may have happened very early (likely >4.5–4.4 billion years), the Moon likely inherited considerable mantle heterogeneity acquired from early magma-ocean processes.

2.6. *Alternatives to the canonical giant-impact models and further testing*

Compared to the canonical giant-impact hypothesis, a Synestia lunar

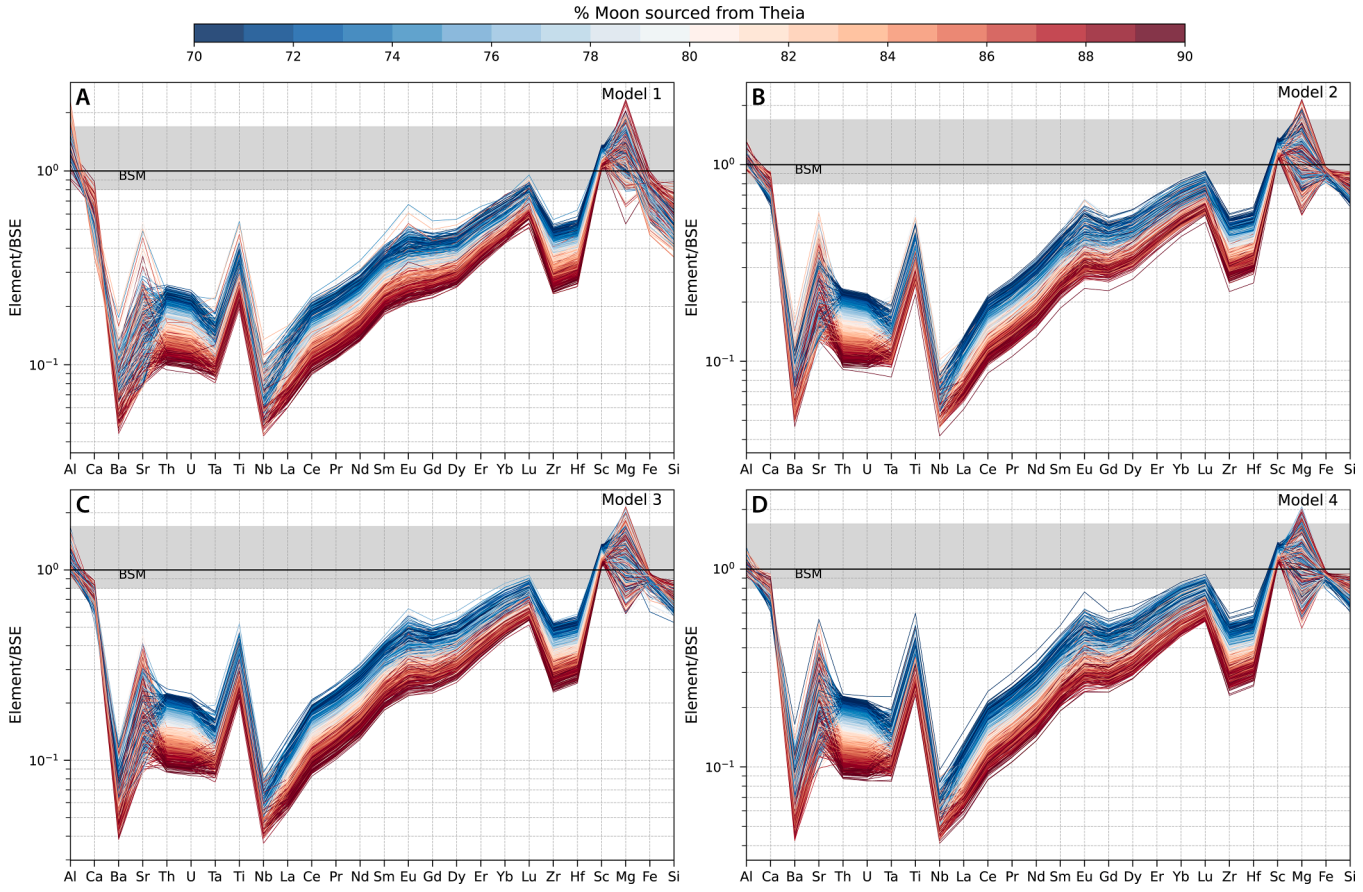

Fig. 10. Comparison of complete refractory element compositions between the canonical giant-impact predictions and lunar observations, assuming mantle overturn in the pre-impact bodies. The y-axis data show the modeled element concentrations of the BSM normalized by the BSE values. The horizontal line and shaded envelope represent the observed BSM composition, which is consistent with the BSE and with a ~10 % uncertainty (Fu and Jacobsen, 2024; Taylor and Wieczorek, 2014). Each panel corresponds to results derived from a specific sampling model, as shown in Figs. 4 and 5. Each color-coded curve (1000 curves per panel) represents one simulation of the modeled BSM element composition based on the percentage of the Moon's material sourced from Theia. Mantle overturn preceding the giant impact would result in strongly depleted refractory element concentrations and fractionated elemental ratios relative to the BSM constraints.

origin provides a straightforward solution to explain the near-identical refractory elemental and isotopic compositions of the Earth and Moon (Lock et al., 2018). Other disk equilibration models, including turbulent mixing through liquid-vapor exchange (Pahlevan and Stevenson, 2007; Pahlevan et al., 2010) and magnetorotational instability (MRI)-driven turbulence (e.g., Charnoz and Michaut, 2015; Gammie et al., 2016), are unclear regarding their efficiency at homogenizing refractory lithophile elements between the Earth and the lunar disk.

These disk-equilibration processes require extremely high temperatures (>4000 K) to vaporize refractory elements at lunar-disk-relevant vapor pressures (Fegley et al., 2023; Ivanov et al., 2022; Lock et al., 2018) to permit mixing. Partial vaporization of refractory elements would introduce additional elemental and isotopic fractionation between the BSE and BSM, which is inconsistent with current observations. Furthermore, achieving the required extent of mixing in such disk-equilibration models would be particularly challenging under a canonical giant-impact scenario, given the predicted remarkable difference in the initial refractory element compositions between the lunar debris disk and the post-impact Earth (Fig. 7). The hypothesis of a shallow MO on the proto-Earth preceding the giant impact, where the Moon is primarily sourced from this MO (Hosono et al., 2019), also makes it hard to explain the observed lunar refractory element compositions. A shallow, residual proto-Earth MO was likely chemically fractionated relative to the BSE composition due to solid-melt element partitioning (see Fig. 2A for an example),and sampling of this layer would result in a chemically distinct BSM composition from the BSE.

Besides element ratio and concentration variations as test sets, resolvable mass-dependent stable isotope heterogeneity for refractory elements within planetary interiors has also been increasingly recognized, warranting systematic implementation in Moon-formation testing. Taking Ca stable isotopes as an example, $\delta^{44/40}$Ca heterogeneity in various mantle source regions has been inferred for Vesta (Zhu et al., 2023), the Moon (Fu et al., 2023; Klaver et al., 2021; Simon and DePaolo, 2010; Simon et al., 2017; Valdes et al., 2014), Mars (Magna et al., 2015), and Earth (Eriksen and Jacobsen, 2022; Eriksen et al., 2024). Analogous to the refractory element proxies examined in this study, mass-dependent isotopic variations could serve as complementary tools for testing specific giant-impact models, although the magnitude of isotopic fractionation is generally smaller (fractionation at sub per-mil levels). Nevertheless, the successful preservation of such small yet resolvable heterogeneity in planetary interiors hints at a possible lack of efficient early mantle compositional mixing in the Solar System bodies, providing supporting evidence for evaluating mantle heterogeneity for the pre-impact bodies.

Lastly, obtaining high-resolution data on the original locations of disk materials within the pre-impact bodies from smoothed-particle hydrodynamic (SPH) canonical giant-impact simulations (e.g., Canup et al., 2004; Hull et al., 2024; Nakajima and Stevenson, 2015) would enable more rigorous testing of the feasibility of this class of models. Beyond its implications for Moon formation, this work highlights the potential for applying such an interconnected geochemical-geophysical framework, which leverages detailed pre-impact element distribution and post-impact redistribution, to explore other planet–moon formation processes potentially linked to giant-impact events (e.g., Kovačević

et al., 2022; Lock and Stewart, 2017; Stewart and Leinhardt, 2011).

3. Conclusions

In the Moon-forming giant-impact scenario, the internal compositional heterogeneity of the pre-impact bodies and the impact-driven sampling should collectively shape the initial composition of the lunar disk. However, these two key parameter spaces have yet to be jointly incorporated into a unified numerical framework for evaluating lunar origin models. Here, we present a new modeling approach that integrates both dimensions of constraint to further test competing Moon-formation hypotheses. We apply this framework to the canonical giant-impact model, which preferentially samples the shallow silicate mantles of the colliding bodies to form the proto-lunar disk. Our modeling shows that the canonical model predicts a highly fractionated disk composition relative to Earth's—in both refractory element concentrations and ratios—posing a challenge to explaining the near-identical Earth–Moon refractory element composition. Instead, the observed similarity implies a need for extensive post-impact homogenization of the disk, an outcome more feasibly achieved under a high-energy impact scenario such as the Synestia model. Our framework offers a promising avenue for future investigations, including integration with thermo-chemical mantle heterogeneity models, high-resolution dynamical simulations, and the giant-impact formation of other planetary bodies.

CRediT authorship contribution statement

Hairuo Fu: Writing – review & editing, Writing – original draft, Visualization, Validation, Software, Resources, Project administration, Methodology, Investigation, Formal analysis, Conceptualization. **Stein B. Jacobsen:** Writing – review & editing, Validation, Supervision, Project administration, Funding acquisition.

Declaration of competing interest

The authors declare that they have no known competing financial interests or personal relationships that could have appeared to influence the work reported in this paper.

Acknowledgments

This work was partly funded by DOE NNSA-SSAA grant DE-NA0004084 (to S.B.J., principal investigator). We thank two anonymous reviewers for their constructive and helpful comments. We are also thankful to Jesse Gu, Eugenia Hyung, Robin Canup, and Paul Warren for valuable discussions.

Supplementary materials

Supplementary material associated with this article can be found, in the online version, at doi:10.1016/j.epsl.2025.119697.

Data availability

The authors declare that the data supporting the findings of this study are available within the article and its Supplementary Material files.

References

Alexander, C.M., 2019a. Quantitative models for the elemental and isotopic fractionations in the chondrites: the non-carbonaceous chondrites. Geochim. Cosmochim. Acta 254, 246–276.
Alexander, C.M., 2019b. Quantitative models for the elemental and isotopic fractionations in chondrites: the carbonaceous chondrites. Geochim. Cosmochim. Acta 254, 277–309.
Barboni, M., et al., 2017. Early formation of the Moon 4.51 billion years ago. Sci. Adv. 3, 1602365.
Boukaré, C., Badro, J., Samuel, H., 2025. Solidification of Earth's mantle led inevitably to a basal magma ocean. Nature 640, 114–119.
Boukaré, C.E., Parmentier, E.M., Parman, S.W., 2018. Timing of mantle overturn during magma ocean solidification. Earth. Planet. Sci. Lett. 491, 216–225.
Budde, G., Burkhardt, C., Kleine, T., 2019. Molybdenum isotopic evidence for the late accretion of outer Solar System material to Earth. Nat. Astron. 3, 736–741.
Canup, R.M., Asphaug, E., 2001. Origin of the Moon in a giant impact near the end of the Earth's formation. Nature 412, 708–712.
Cano, E.J., Sharp, Z.D., Shearer, C.K., 2020. Distinct oxygen isotope compositions of the Earth and Moon. Nat. Geosci. 13, 270–274.
Canup, R.M., 2004. Simulations of a late lunar-forming impact. Icarus 168, 433–456.
Canup, R.M., 2012. Forming a moon with an earth-like composition via a giant impact. Science 338, 1052–1055.
Canup, R.M., Righter, K., Dauphas, N., Pahlevan, K., Ćuk, M., Lock, S.J., et al., 2023. Origin of the moon. Rev. Mineral. Geochem. 89 (1), 53–102.
Carlson, R.W., Boyet, M., 2008. Composition of the Earth's interior: the importance of early events. Philos. Trans. R. Soc. A 366, 4077–4103.
Caro, G., Bourdon, B., Wood, B.J., Corgne, A., 2005. Trace-element fractionation in Hadean mantle generated by melt segregation from a magma ocean. Nature 436, 246–249.
Charnoz, C., Michaut, C., 2015. Evolution of the protolunar disk: dynamics, cooling timescale and implantation of volatiles onto the Earth. Icarus 260, 440–463.
Ćuk, M., Stewart, S.T., 2012. Making the moon from a fast-spinning Earth: a giant impact followed by resonant despinning. Science 338, 1047–1052.
Dauphas, N., Burkhardt, C., Warren, P.H., Teng, F.-Z., 2014. Geochemical arguments for an Earth-like Moon-forming impactor. Phil. Trans. R. Soc. A 372, 20130244.
Day, J.M., Paquet, M., Udry, A., Moynier, F., 2024. A heterogeneous mantle and crustal structure formed during the early differentiation of Mars. Sci. Adv. 10, eadn9830.
Elkins-Tanton, L.T., Parmentier, E.M., Hess, P.C., 2003. Magma ocean fractional crystallization and cumulate overturn in terrestrial planets: implications for Mars. Meteorit. Planet. Sci. 38, 1753–1771.
Elkins-Tanton, L.T., 2008. Linked magma ocean solidification and atmospheric growth for Earth and Mars. Earth. Planet. Sci. Lett. 271, 181–191.
Elkins-Tanton, L.T., 2012. Magma oceans in the inner solar system. Annu Rev. Earth. Planet. Sci. 40, 113–139.
Eriksen, Z.T., Jacobsen, S.B., 2022. Calcium isotope constraints on OIB and MORB petrogenesis: the importance of melt mixing. Earth. Planet. Sci. Lett. 593, 117665.
Eriksen, Z.T., Jacobsen, S.B., Day, J.M., White, W.M., 2024. Calcium isotope variability among ocean islands reveals the physical and lithological controls on mantle partial melting. Geochim. Cosmochim. Acta 375, 326–341.
Fegley, B.J., Lodders, K., Jacobson, N.S., 2023. Chemical equilibrium calculations for bulk silicate earth material at high temperatures. Geochemistry 83, 125961.
Fischer, M., Peters, S.T.M., Herwartz, D., Hartogh, P., Di Rocco, T., Pack, A., 2024. Oxygen isotope identity of the Earth and Moon with implications for the formation of the Moon and source of volatiles. PNAS 52, e2321070121.
Fischer, R.A., Zube, N.G., Nimmo, F., 2021. The origin of the Moon's Earth-like tungsten isotopic composition from dynamical and geochemical modeling. Nat. Commun. 12.
Fu, H., Jacobsen, S.B., Sedaghatpour, F., 2023. Moon's high-energy giant-impact origin and differentiation timeline inferred from Ca and Mg stable isotopes. Commun. Earth. Environ. 4, 307.
Fu, H., Jacobsen, S.B., 2024. Earth-moon refractory element similarity constrains a thoroughly- mixed Moon-forming disk. Earth. Planet. Sci. Lett. 646, 119008.
Gammie, C.F., Liao, W., Ricker, P.M., 2016. A hot Big Bang theory: magnetic fields and the early evolution of the protolunar disk. Astrophys. J. 828.
Greenwood, R.C., Barrat, J., Yamaguchi, A., Franchi, I.A., Scott, E.R., Bottke, W.F., Gibson, J., 2014. The oxygen isotope composition of diogenites: evidence for early global melting on a single, compositionally diverse, HED parent body. Earth. Planet. Sci. Lett. 390, 165–174.
Greer, J., Zhang, B., Isheim, D., Seidman, D.N., Bouvier, A., Heck, P.R., 2023. 4.46 Ga zircons anchor chronology of lunar magma ocean. Geochem. Perspect. Lett. 27, 49–53.
Harper Jr., C.L., Jacobsen, S.B., 1996. Noble gases and Earth's accretion. Science 273, 1814–1818.
Hosono, N., Karato, S., Makino, J., Saitoh, T.R, 2019. Terrestrial magma ocean origin of the Moon. Nat. Geosci. 12, 418–423.
Hess, P.C., Parmentier, E.M., 1995. A model for the thermal and chemical evolution of the Moon's interior: implications for the onset of mare volcanism. Earth. Planet. Sci. Lett. 134, 501–514.
Hull, S.D., Nakajima, M., Hosono, N., Canup, R.M., Gassmöller, R., 2024. Effect of equation of State and cutoff density in smoothed particle hydrodynamics simulations of the moon-forming giant impact. Planet. Sci. J. 5.
Hyung, E., Huang, S., Petaev, M.I., Jacobsen, S.B., 2016. Is the mantle chemically stratified? Insights from sound velocity modeling and isotope evolution of an early magma ocean. Earth. Planet. Sci. Lett. 440, 158–168.
Hyung, E., Jacobsen, S.B., 2020. The $^{142}Nd/^{144}Nd$ variations in mantle-derived rocks provide constraints on the stirring rate of the mantle from the Hadean to the present. Proc. Natl. Acad. Sci. 117, 14738–14744.
Ivanov, D., Fitoussi, C., Bourdon, B., 2022. Trace element volatility and the conditions of liquid-vapor separation in the proto-lunar disk. Icarus 386, 115143.
Jacobsen, S.B., Yu, G., 2015. Extinct isotope heterogeneities in the mantles of Earth and Mars: Implications for mantle stirring rates. Meteorit. Planet. Sci. 50 (4), 555–567.
Khan, A., Maclennan, J., Taylor, S.R., Connolly, J.A., 2006. Are the Earth and the Moon compositionally alike? Inferences on lunar composition and implications for lunar origin and evolution from geophysical modeling. J. Geophys. Res. 111.

Klaver, M., Luu, T., Lewis, J.T., Jansen, M.N., Anand, M., Schwieters, J.B., Elliott, T., 2021. The Ca isotope composition of mare basalts as a probe into the heterogeneous lunar mantle. Earth. Planet. Sci. Lett. 570, 117079.
Kovacevic, T., González-Cataldo, F., Stewart, S.T., Militzer, B., 2022. Miscibility of rock and ice in the interiors of water worlds. Sci. Rep. 12.
Kronrod, E.V., Kronrod, V., Kuskov, O.L., Nefedyev, Y.A., 2018. Geochemical constraints for the bulk composition of the moon. Dokl. Earth Sci. 483, 1475–1479.
Kruijer, T.S., Kleine, T., Fischer-Gödde, M., Sprung, P., 2015. Lunar tungsten isotopic evidence for the late veneer. Nature 520, 534–537.
Lock, S.J., Stewart, S.T., 2017. The structure of terrestrial bodies:impact heating, corotation limits, and synestias. J. Geophys. Res. Planets. 122, 950–982.
Lock, S.J., Stewart, S.T., Petaev, M.I., Leinhardt, Z., Mace, M.T., Jacobsen, S.B., Ćuk, M., 2018. The origin of the Moon within a terrestrial synestia. J. Geophys. Res.: Planets 123, 910–951.
Lock, S.J., Bermingham, K.R., Parai, R., Boyet, M., 2020. Geochemical constraints on the origin of the moon and preservation of ancient terrestrial heterogeneities. Space Sci. Rev. 216.
Magna, T., Gussone, N., Mezger, K., 2015. The calcium isotope systematics of Mars. Earth. Planet. Sci. Lett. 430, 86–94.
McDonough, W.F., Sun, S.S., 1995. The composition of the Earth. Chem. Geol. 120, 223–253.
Nakajima, M., Stevenson, D.J., 2015. Melting and mixing states of the Earth's mantle after the Moon-forming impact. Earth. Planet. Sci. Lett. 427, 286–295.
O'Brien, D.P., Walsh, K.J., Morbidelli, A., Raymond, S.N., Mandell, A.M., 2014. Water delivery and giant impacts in the 'Grand Tack' scenario. Icarus 239, 74–84.
Pahlevan, K., Stevenson, D.J., 2007. Equilibration in the aftermath of the lunar-forming giant impact. Earth. Planet. Sci. Lett. 262, 438–449.
Pahlevan, K., Stevenson, D.J., Eiler, J.M., 2010. Chemical fractionation in the silicate vapor atmosphere of the Earth. Earth. Planet. Sci. Lett. 301, 433–443.
Schmidt, M.W., Kraettli, G., 2022. Experimental crystallization of the lunar magmaocean, initial selenotherm and density stratification, and implications for crust formation, overturn and the bulk silicate moon composition. J. Geophys. Res. 127.
Simon, J.I., DePaolo, D.J., 2010. Stable calcium isotopic composition of meteorites and rocky planets. Earth. Planet. Sci. Lett. 289, 457–466.
Simon, J.I., Jordan, M.K., Tappa, M.J., Schauble, E.A., Kohl, I.E., Young, E.D., 2017. Calcium and titanium isotope fractionation in refractory inclusions: tracers of condensation and inheritance in the early solar protoplanetary disk. Earth. Planet. Sci. Lett. 472, 277–288.
Stähler, S.C., Khan, A., Banerdt, W.B., Lognonné, P.H., Giardini, D., Ceylan, S., Drilleau, M., Duran, A.C., Garcia, R.F., Huang, Q., Kim, D., Lekić, V., Samuel, H., Schimmel, M., Schmerr, N.C., Sollberger, D., Stutzmann, É., Xu, Z., Antonangeli, D., Charalambous, C., Davis, P.M., Irving, J.C., Kawamura, T., Knapmeyer, M., Maguire, R.R., Marusiak, A.G., Panning, M.P., Perrin, C., Plesa, A.C., Rivoldini, A., Schmelzbach, C., Zenhäusern, G., Beucler, É., Clinton, J.F., Dahmen, N.L., van Driel, M., Gudkova, T., Horleston, A.C., Pike, W.T., Plasman, M., Smrekar, S.E., 2021. Seismic detection of the martian core. Science 373, 443–448.
Stewart, S.T., Leinhardt, Z.M., 2011. Collisions between gravity-dominated bodies. II. The diversity of impact outcomes during the end stage of planet formation. Astrophys. J. 751.
Taylor, S.R., 1982. Planetary science: a lunar perspective. Lunar Planet. Inst. 502.
Taylor, G.J., Wieczorek, M.A., 2014. Lunar bulk chemical composition: a post-Gravity Recovery and Interior Laboratory reassessment. Philos. Trans. R. Soc. A 372.
Thiemens, M.M., Sprung, P., Fonseca, R.O., Leitzke, F.P., Muünker, C., 2019. Early Moon formation inferred from hafnium–tungsten systematics. Nat. Geosci. 12, 696–700.
Valdes, M.C., Moreira, M.A., Foriel, J., Moynier, F., 2014. The nature of Earth's building blocks as revealed by calcium isotopes. Earth. Planet. Sci. Lett. 394, 135–145.
Warren, P.H., 2005. New' lunar meteorites: implications for composition of the global lunar surface, lunar crust, and the bulk Moon. Meteorit. Planet. Sci. 40, 477–506.
Wieczorek, M.A., Jolliff, B.L., Khan, A., Pritchard, M.E., Weiss, B.P., Williams, J.G., et al., 2006. The constitution and structure of the lunar interior. Rev. Mineral. Geochem. 60 (1), 221–364.
Wood, J.A., Dickey, J.S.J., Marvin, U.B., 1970. Powell lunar anorthosites and a geophysical model of the moon. Proc. Apollo 11 Lunar Sci. Conf. 965–988.
Yoshizaki, T., McDonough, W.F., 2019. The composition of Mars. Geochim. Cosmochim. Acta 273, 137–162.
Young, E.D., Kohl, I.E., Warren, P.H., Rubie, D.C., Jacobson, S.A., Morbidelli, A., 2016. Oxygen isotopic evidence for vigorous mixing during the moon-forming giant impact. Science 351, 493–496.
Yu, G., Jacobsen, S.B., 2011. Fast accretion of the Earth with a late Moon-forming giant impact. Proc. Natl. Acad. Sci. USA 108, 17604–17609.
Zhang, J., Dauphas, N., Davis, A., Leya, I., Fedkin, A., 2012. The proto-Earth as a significant source of lunar material. Nat. Geosci. 5, 251–255.
Zhu, K., Hui, H., Klaver, M., Li, S.-J., Chen, L., Hsu, W., 2023. Calcium isotope evolution during differentiation of Vesta and calcium isotopic heterogeneities in the inner solar system. Geophys. Res. Lett. 50, e2022GL102179.